Journal of Alloys and Compounds, 211/212 (1994) 576–580
JALCOM 068

Giant magnetostrictive materials: thin film formation and application to magnetic surface acoustic wave devices

H. Uchida, M. Wada and K. Koike
Department of Applied Physics, Tokai University, 1117 Kita-Kaname, Hiratsuka, Kanagawa 259-12 (Japan)

H.H. Uchida
Department of Resources and Environmental Sciences, Tokai University, 1117 Kita-Kaname, Hiratsuka, Kanagawa 259-12 (Japan)

V. Koeninger and Y. Matsumura
Kanagawa Academy of Science and Technology, Sakado, Takatsu, Kawasaki, Kanagawa 213 (Japan)

H. Kaneko and T. Kurino
Society of Non-Traditional Technology, 1-2-8 Toranomon, Minato-ku, Tokyo 105 (Japan)

Abstract

This paper points out current problems in the research and development of giant magnetostrictive materials (GMMs), and the use of thin film GMMs instead of bulk is emphasized because of the ready and inexpensive production and high applicability. One of the most prominent applications using GMM films is the magnetic surface acoustic wave device with tunability under an external magnetic field. Thin films of the giant magnetostrictive $Tb_{0.3}Dy_{0.7}Fe_2$ alloy were prepared by vacuum flash evaporation. The film structure was able to be changed from amorphous to crystalline by controlling the substrate temperature and deposition rate. The crystalline films exhibited much higher magnetization and larger magnetostrictions than did the amorphous films. The contamination of the films in vacuum facilitated amorphization and markedly reduced the magnetostrictions of the films. X-ray diffraction and Auger electron spectroscopy analyses revealed that the ratio of vacuum to deposition rate is an appropriate indicator to assess the contamination effect of films.

1. Introduction

Magnetostriction is a well-known phenomenon of magnetoelastic coupling which exhibits a change in dimension and a change in the elastic modulus of a magnetic material. In the applications of magnetostrictive materials, a high magnetization is important for high efficiency in transducing electrical to magnetic energy in the materials. In addition, a high saturation magnetostriction and a low magnetic anisotropy for less hysteretic magnetization are desirable. $TbFe_2$ and $DyFe_2$ have large positive magnetostriction values and opposite signs of magnetic anisotropy. On the basis of this, the highly magnetostrictive $Tb_{0.3}Dy_{0.7}Fe_2$ alloy (Terfenol-D) was synthesized [1]. Intensive efforts have yielded many interesting applications of giant magnetostrictive materials (GMMs) exhibiting magnetostrictions over 1000 ppm [2]. Also, in other groups of materials, very high magnetostrictions were found. Recently, large magnetostriction of the order of 10^{-4} for a single crystal of $Bi_2Sr_2CaCu_2O_8$ has been reported [3]. Thus the fundamental investigation of many different substances seems to be of great importance to understand the mechanism of magnetoelastic interactions yielding giant magnetostriction. However, in spite of the interesting features, the utilization and commercialization of bulk GMMs seems to be strongly limited at present. One of the serious issues for this is the expensive production of bulk GMMs. The formation of pseudobinary RFe_2 ($R \equiv$ rare earths) intermetallics proceeds through complicated peritectic transformations. An alternative process such as the melt-spinning method [4] seems to be necessary for reduction in costs and the expansion in the utilization of GMMs [5].

One alternative way may be the use of thin film GMMs because of the following advantages: (1) simple production process with respect to controlling composition and structure compared with those of bulk GMMs, resulting in inexpensive production; (2) ready connection with conventional semiconductor devices; (3) new functions and applications resulted from two-dimensional magnetoelastic interactions in the film.

From this point of view, we investigated the preparation of magnetic surface acoustic wave (MSAW)

SSDI 0925-8388(93)00068-A

devices with thin film GMMs using four different processes: vacuum flash evaporation, activated reactive evaporation, electron beam evaporation and ion beam sputter with a plasma filament. The details of these different processes have been reported elsewhere [6–10]. The greatest advantage of an MSAW device is the tunability obtained by controlling the external magnetic field [11]. Much work was done using Ni films [12, 13]. The high magnetostriction and high ΔE effect of the GMMs led one to expect high tunability of devices using these films instead of Ni films. This paper reports fundamental data such as the formation of GMM thin films by the flash evaporation process, the magnetization and the magnetostriction measured for the films.

2. Experimental processes

2.1. Deposition

The purities of Tb, Dy and Fe used were of the order of 99.9–99.99%. These elements were arc melted in Ar to produce $TbFe_2$ and $DyFe_2$ block samples. The structures of the samples were examined by Mo Kα X-ray diffraction (XRD). The compositions of the samples were analyzed by inductively coupled plasma spectroscopy (ICPS) and energy-dispersive X-ray spectroscopy (EDXS). The block samples were cyclically hydrided and dehydrided, which reproducibly yielded $TbFe_2$ and $DyFe_2$ powders with a mean particle size below 10 μm. The details of the pulverization process of rare earth (R)–transition metal alloys by cyclic hydriding treatment have been described elsewhere [14, 15]. The $TbFe_2$ and $DyFe_2$ powders produced were mixed and subjected to flash evaporation, so that the film formed should have the composition $Tb_{0.2-0.3}Dy_{0.7-0.8}Fe_2$. The compositions of these alloy films are denoted as (Tb, Dy)Fe_2 in this paper. The difference between the compositions of the powder and formed film samples was within 5 at.%. The details of the system used have been reported elsewhere [6, 16]. The film samples were deposited onto silica glass, copper or tungsten substrates supported by a hemispheric rotator above a tungsten heater, maintained at over 2300 K, on which the powders were evaporated. The substrate temperature was varied from 400 to 650 K. The background pressure of the system used was changed from 6.9×10^{-5} to 1.3×10^{-3} Pa. The deposition rate was changed from 1.3 to 24 Å s^{-1}. The thickness of film samples was in the range from 4000 to 9000 Å. The ratio r (Pa s $Å^{-1}$) of the vacuum to the deposition rate was a useful parameter to assess the contamination of the film formed. The details of the relation of r to the contamination effect have been reported elsewhere [16, 17]. The deposited films were examined with respect to the structure using XRD and the composition using ICPS, EDXS and Auger electron spectroscopy (AES).

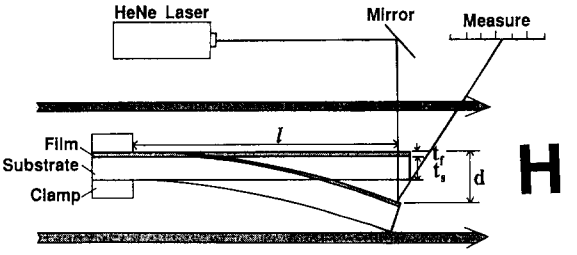

Fig. 1. Experimental arrangement for the measurement of magnetostrictions using a bending method [18].

2.2. Measurements of magnetization and magnetostriction

The prepared film samples were subjected to the measurement of magnetizations parallel and perpendicular to the samples as a function of magnetic field using a vibrating-sample magnetometer. Subsequently the magnetostrictions λ parallel to H were measured by measuring the bending d of a substrate covered with a GMM film, as shown in Fig. 1. An He–Ne laser beam was reflected from the sample onto a scale. The displacement of the beam spot on the scale by the bending of the sample was measured and λ for the sample was calculated using the following equation [18]:

$$\lambda = d\,\frac{t_s^2}{3t_f l^2}\,\frac{E_s(1+\nu_f)}{E_f(1-\nu_s)} = \frac{\Delta l}{l}$$

where l is the length of the sample, t_f and t_s are the thicknesses of the film and substrate respectively, E_f and E_s are Young's moduli for the film and substrate respectively, and ν_f and ν_s are Poisson's ratios for the film and substrate respectively. Here, $d \ll t_f + t_s$ and $t_s \gg t_f$ are assumed. The details of this bending method have been reported elsewhere [8].

3. Results and discussions

3.1. Effect of preparation conditions on the film structure and composition

Figure 2 shows the typical XRD patterns of an amorphous-like film (film A) deposited at $r = 1.4\times10^{-5}$ Pa s $Å^{-1}$ and 405 K, an amorphous-like and rather contaminated film (film B) deposited at $r = 2.4\times10^{-4}$ Pa s $Å^{-1}$ and 626 K and a crystalline film (film C) deposited at $r = 4.8\times10^{-5}$ Pa s $Å^{-1}$ and 610 K. These results indicate that the preparation parameters such as deposition rate and vacuum have marked influences on the film structure. The effect of the preparation conditions on the structures of (Tb, Dy)Fe_2 films were assessed by substrate temperature and the ratio r of vacuum to deposition rate, as summarized in Fig. 3.

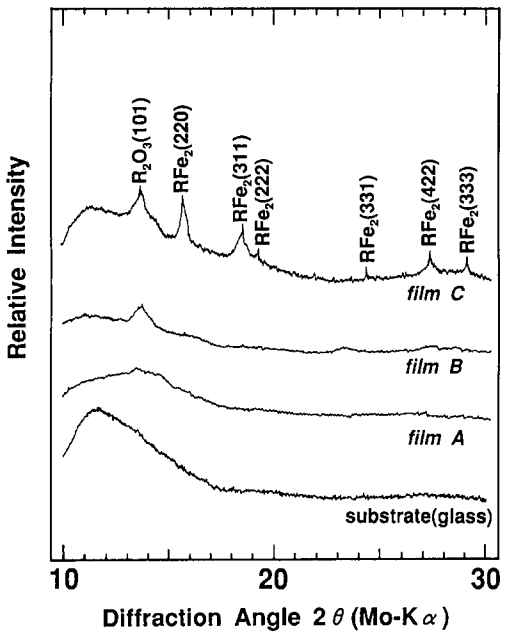

Fig. 2. XRD (Mo Kα) patterns of film A ($r=1.4\times10^{-5}$ Pa s Å^{-1} and 405 K), film B ($r=2.4\times10^{-4}$ Pa s Å^{-1} and 626 K), film C ($r=4.8\times10^{-5}$ Pa s Å^{-1} and 610 K) and substrate (glass).

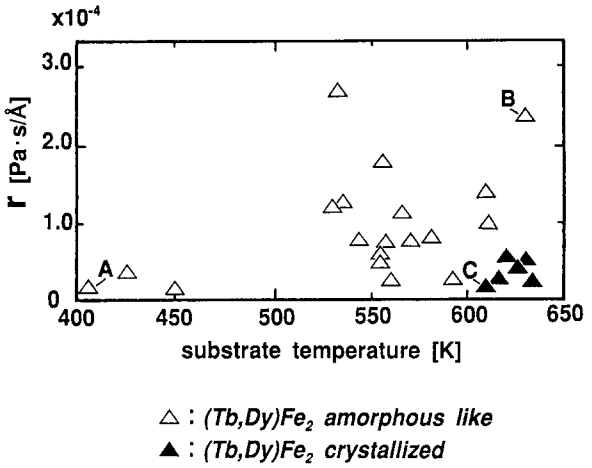

Fig. 3. Influences of the preparation conditions, namely the vacuum-to-deposition ratio and the substrate temperature, on the structure of the films deposited.

By lowering r, the occlusion of impurities in samples, namely the contamination effect becomes less [6, 16, 17]. From the results of XRD, the crystalline and amorphous-like films are designated as full triangles and open triangles respectively, as shown in Fig. 3. When the substrate temperature was lower than 600 K, the film became amorphous like (film A). Crystalline (Tb, Dy)Fe_2 films could be obtained when r was lower than 7×10^{-5} Pa s Å^{-1} and the substrate temperature was higher than 600 K. When r became higher, the film structure (film B) remains amorphous like even at 626 K, as shown in Fig. 2. The occlusion of impurities during deposition may hinder the recovery of high

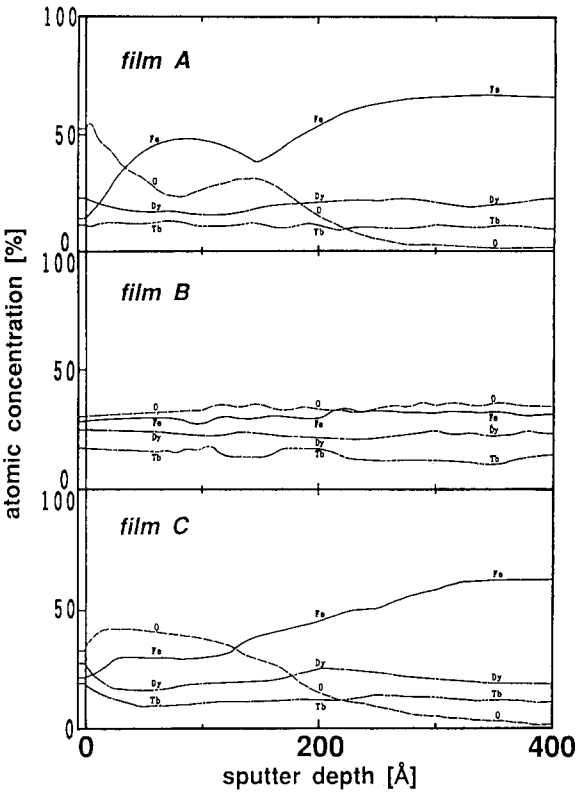

Fig. 4. AES depth profiles of films A, B and C deposited under the preparation conditions corresponding to those in Fig. 2.

density of dislocations and the recrystallization, resulting in an amorphous-like or disordered state of the film even at temperatures higher than 600 K.

Figure 4 shows the AES depth profiles of films A, B and C. These samples were analyzed after air exposure for 4 months. Films A and C deposited at a low r value exhibit the composition $Tb_{0.3}Dy_{0.7}Fe_2$ at a depth over 200–300 Å although the occurrence of surface oxidation and corresponding compositional alterations can be seen only at the surface regions. Film B deposited at a high r value exhibits no drastic surface oxidation; however, the oxygen amount predominates over Tb, Dy and Fe and remains almost constant throughout the sample. This means that a high rate of oxidation took place during the deposition process. This is consistent with the XRD result in Fig. 2 where the presence of an R_2O_3 XRD line can be seen. Although a similar oxide XRD line can be seen for film C, the oxidation is limited to the surface region as the AES depth profile indicates.

3.2. Magnetization and magnetostriction

Figure 5(a), (b) and (c) shows the typical curves of magnetization I (e.m.u. cm^{-3}) *vs.* applied magnetic field H (kOe) of the (Tb, Dy)Fe_2 films A, B and C respectively. The I–H curves display the measured magnetizations of the film perpendicular to H (curves

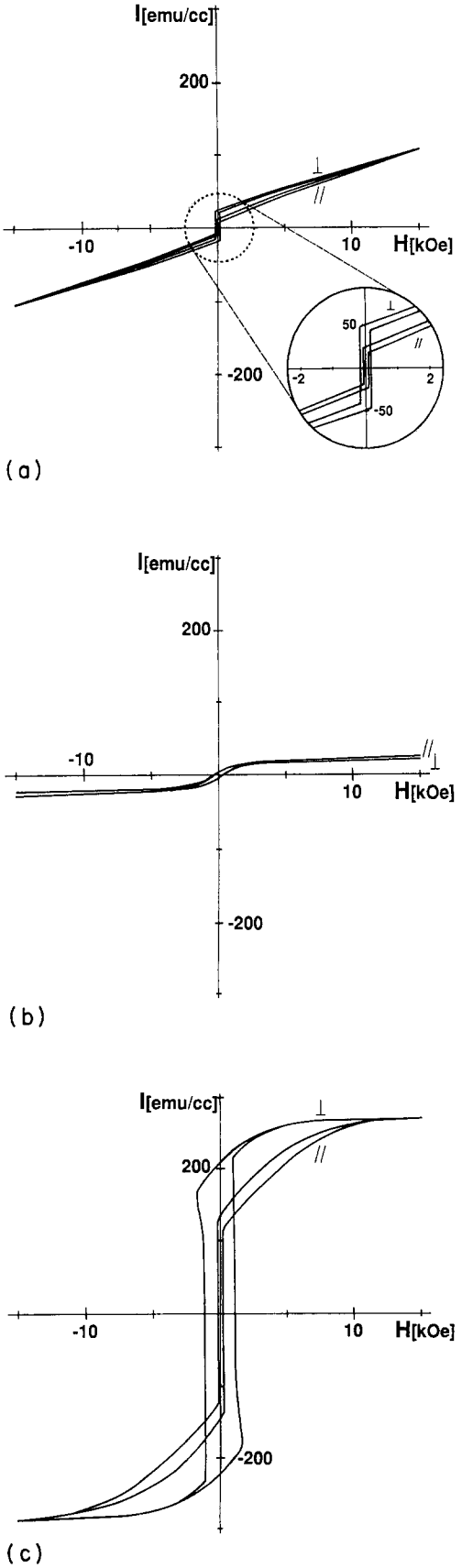

Fig. 5. Magnetization curves of the films: (a) film A; (b) film B; (c) film C.

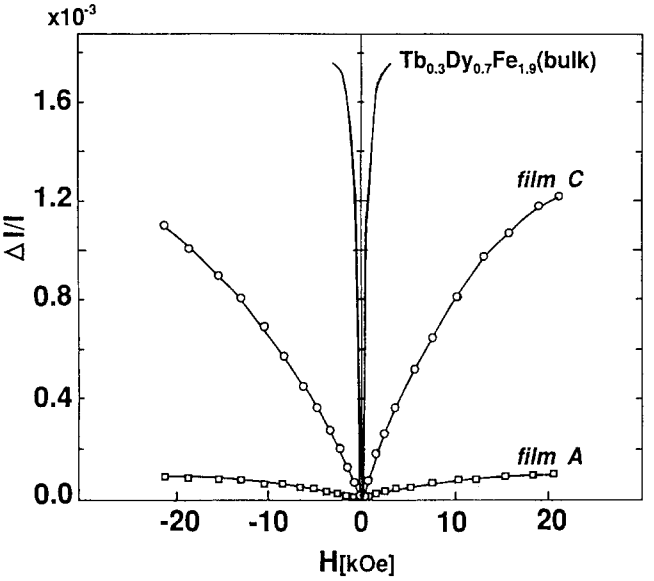

Fig. 6. Magnetostrictions of the films A and B and a bulk sample.

labelled $\perp$) and parallel to H (curves labelled $\parallel$). Figure 5(a) and (b) shows the typical I–H curves for amorphous (Tb, Dy)Fe_2 films as shown by the XRD pattern in Fig. 3(a) and (b) respectively. The amorphous films yield much smaller saturation magnetizations than does the crystalline film C. The crystalline film C and amorphous film A were formed at a similar deposition condition with respect to r. These conditions suggest that films A and C are relatively clean compared with film B. For film A, the smaller magnetization and less magnetic anisotropy may be ascribed not to a contamination effect but rather to the disordered structure and residual strains in the film accumulated at a lower substrate temperature. These defects may cause locally disordered magnetic anisotropy and disordered spin orientations, resulting in a smaller and rather isotropic magnetization. For film B, marked oxidation during the deposition process seems to be responsible for the low response to magnetic fields.

The magnetostrictions measured for films A and C are shown in Fig. 6 and compared with that of a bulk sample. In accordance with the residual magnetizations, film C exhibits a much higher saturation magnetostriction parallel to the magnetic field than film A does. These magnetostrictions, 10^{-4}–10^{-3}, are smaller than that of a bulk sample; however, they are still large compared with those of conventional magnetostrictive materials such as Fe and Ni, which have magnetostrictions of the order of 10^{-6}–10^{-5}.

4. Conclusions

The (Tb, Dy)Fe_2 films can be prepared by a flash evaporation process and exhibit large magnetostrictions

of the order of 10^{-4}–10^{-3}. The magnetostrictive response, such as hysteresis under an applied magnetic field, is quite similar to the *I–H* curves. The films prepared in this work exhibited a surface acoustic wave (SAW) velocity change of 0.1% at 20 MHz and the response of the velocity change to the external magnetic field was around 10^{-4}% kOe^{-1} [10]. These values are markedly influenced by the film preparation conditions, the strains and the film thickness. Therefore systematic investigations are being undertaken in order to find the factors affecting the magnetic properties and the SAW velocity: intrinsic factors such as structure, composition and film thickness, and extrinsic factors such as contamination, strains, film–substrate interface matching and frequency dependence.

References

1 A.E. Clark, in E.P. Wohlfarth (ed.), *Ferromagnetic Materials*, Vol. 1, North-Holland, Amsterdam, 1980, Chapter 7.

2 A.E. Clark, *Proc. Int. Conf. on Giant Magnetostrictive Materials and Their Applications, Tokyo, November 1992*, Advanced Machining Technology and Development Association, Minato-ku, Tokyo, 1992, p. 9.

3 K. Kitazawa, H. Ikuta, N. Hirota, Y. Nakayama and K. Kishio, *Proc. Int. Conf. on Giant Magnetostrictive Materials and Their Applications, Tokyo, November, 1992*, Advanced Machining Technology and Development Association, Minato-ku, Tokyo, 1992, p. 15.

4 T. Uchida and T. Mori, *Proc. Int. Conf. on Giant Magnetostrictive Materials and Their Applications, Tokyo, November 1992*, Advanced Machining Technology and Development Association, Minato-ku, Tokyo, 1992, p. 169.

5 K. Lenz, *Proc. Int. Conf. on Giant Magnetostrictive Materials and Their Applications, Tokyo, November 1992*, Advanced Machining Technology and Development Association, Minato-ku, Tokyo, 1992, p. 69.

6 H. Uchida, I. Okuyama, M. Wada, H.H. Uchida, Y. Matsumura, V. Koeninger, U. Koike, K. Kamada, T. Kurino and H. Kaneko, *Proc. Int. Conf. on Giant Magnetostrictive Materials and Their Applications, Tokyo, November 1992*, Advanced Machining Technology and Development Association, Minato-ku, Tokyo, 1992, p. 137.

7 H.H. Uchida, H. Uchida, H. Funakura, Y. Matsumura, V. Koeninger and T. Noguchi, *Proc. Int. Conf. on Giant Magnetostrictive Materials and Their Applications, Tokyo, November, 1992*, Advanced Machining Technology and Development Association, Minato-ku, Tokyo, 1992, p. 145.

8 V. Koeninger, Y. Matsumura, T. Noguchi, H.H. Uchida, H. Uchida, H. Funakura, H. Kaneko and T. Kurino, *Proc. Int. Conf. on Giant Magnetostrictive Materials and Their Applications, Tokyo, November 1992,* Advanced Machining Technology and Development Association, Minato-ku, Tokyo, 1992, p. 151.

9 H.H. Uchida, H. Uchida, V. Koeninger, Y. Matsumura, H. Funakura, M. Wada, T. Kurino and H. Kaneko, *J. Alloys Comp.* (1994).

10 V. Koeninger, H.H. Uchida, H. Uchida and Y. Matsumura, *J. Alloys Comp., 211/212* (1994) 581.

11 D.C. Webb, D.W. Forester, A.K. Ganguly and C. Vittoria, *IEEE Trans. Magn., 15* (6) (1979) 1410.

12 R.F. Wiegert and M. Levy, *J. Appl. Phys., 64* (10) (1988) 5411.

13 R.F. Wiegert and M. Levy, *Appl. Phys. Lett., 54* (11) (1989) 995.

14 Y. Matsumura, T. Noguchi, U. Koike, K. Kamada, V. Koeninger, H. Uchida, A. Yamamoto, I. Okuyama, H. Funakura, M. Wada, H.H. Uchida, T. Kurino and H. Kaneko, *J. Magn. Soc. Jpn., 16* (1992) 189.

15 H. Uchida, H.H. Uchida and Y.C. Huang, *J. Less-Common Met., 101* (1984) 459.

16 H. Uchida, K. Kojima, H. Hashimoto and A. Denda, *J. Less-Common Met., 172–174* (1991) 983.

17 H. Uchida, T. Ebisawa, A. Denda, T. Itoh and S. Tsuzuki, *Z. Phys. Chem., N.F., 164* (1989) 1129.

18 A.C. Tam, *IEEE Trans. Magn., 25* (1989) 2629.